Journal of Hydrology, 120 (1990) 1–13
Elsevier Science Publishers B.V., Amsterdam — Printed in The Netherlands

[3]

STUDIES OF A SUBARCTIC COASTAL MARSH. III. MODELLING THE SUBSURFACE WATER FLUXES AND CHLORIDE DISTRIBUTION

JONATHAN S. PRICE[1] and MING-KO WOO[2]

[1]*Department of Geography, Memorial University of Newfoundland, St. John's, Nfld. A1B 3X9 (Canada)*
[2]*Department of Geography, McMaster University, Hamilton, Ont. L8S 4K1 (Canada)*

(Received January 30, 1990; accepted after revision February 10, 1990)

ABSTRACT

Price, J.S. and Woo, M.-k., 1990. Studies of a subarctic coastal marsh. III. Modelling the subsurface water fluxes and chloride distribution. J. Hydrol., 120: 1–13.

A two-dimensional advection dispersion model of solute transport is used to simulate the long-term changes in the chloride distribution of the young isostatically raised beach ridge and depression sequences in a James Bay coastal marsh. The USGS–SUTRA model reproduces the hydraulic conditions in the wetland, causing recharge of freshwater to the ridges and discharge of saline water to the inter-ridge depressions, demonstrating the importance of vertical water fluxes of water and chloride. Even though water velocities are very low, molecular diffusion alone cannot explain the observed chloride distribution. Imposing the characteristics of a frozen surface during winter eliminated the vertical fluxes, and doubled the time required for the simulated chloride distribution to match the field data. The model correctly predicts the observed pattern of suppressed salinity beneath the ridges and a general decrease of salinity with distance inland. The results are useful in understanding the processes which operate in the first 100 years of marsh development.

INTRODUCTION

The emergence of the James Bay coast is the initial phase in the development of one of the largest wetland complexes in the world. Beaches formed on an isostatically prograding shoreline have produced a sequence of progressively older salt marshes interspersed with sub-parallel raised beach ridges. The hydrological behaviour of these coastal marshes is dominated by the ridge and depression topography (Price and Woo, 1988a). The most juvenile ridges present a topographic divide parallel to the coast, but preferential development of organic soils in the wetter topographic depressions raises the water table, causing water to flow over the adjacent coastward ridges (Price and Woo, 1988a).

While overland flow crossing the more mature ridges is important (15% of May–August precipitation), groundwater flow along the regional gradient is only 0.008 mm day^{-1}. However, much higher vertical fluxes of 0.5–0.9 mm day^{-1}

0022-1694/90/$03.50

prompted Price and Woo (1988b) to suggest that recharge of fresh surface water affects the distribution of salt in the marsh. They also found that relict salt occurs in the ancient marine clay underlying the marsh (Price and Woo, 1988c). A numerical model of molecular diffusion (Price and Woo, 1988b) showed that diffusion was important in transporting the relict salt from those low permeability sediments to the more recent marsh sediments, but the model was not able to match the salt distribution in the upper sediments where recharge occurs.

In the absence of strong hydraulic gradients, the vertical distribution of salt in the coastal marsh can be modelled as a Fickian diffusion process as long as the marsh is continuously inundated (Casey and Lasaga, 1987; Price and Woo, 1988b). However, where significant groundwater flow occurs, the chloride concentration will not be estimated correctly without considering advective transport processes. The objective of this study is to simulate the hydrological and solute transport processes in a prograding coastal marsh to predict the chloride distribution, and to understand the processes that govern it. The distribution of salt is important in understanding the spatial patterns of vegetation (Price et al., 1988).

STUDY AREA AND FIELD METHODS

The study site (51°10′N, 79°47′W) located at the southern end of James Bay (Fig. 1), has a continental subarctic climate, with mean January and July

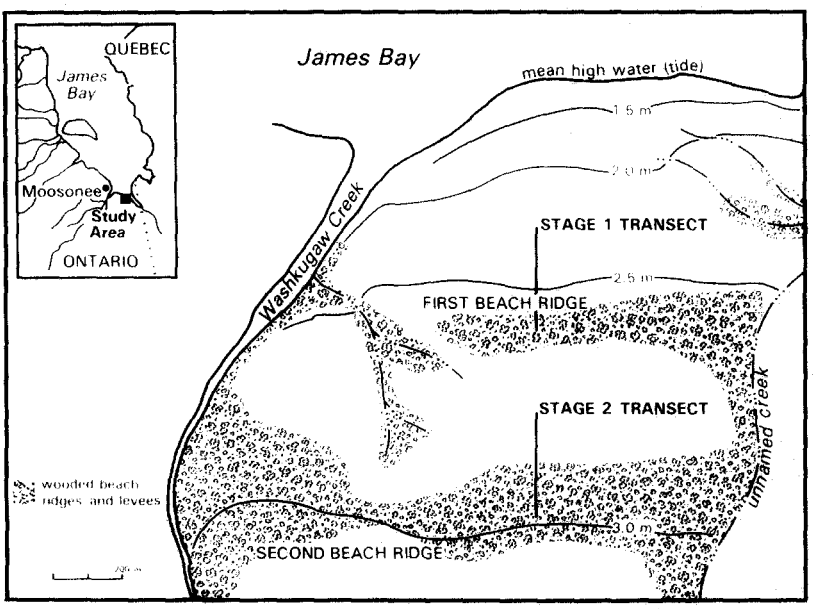

Fig. 1. Study area and transects, indicating the modelled sections.

temperatures at Moosonee, Ontario, of −20.0 and 15.5°C, respectively. Mean annual precipitation is 727 mm, 30% of which falls as snow (Environment Canada, 1982).

Palaeozoic sedimentary bedrock underlies marine silty clay which contains fossil salt deposited during the Tyrrell Sea episode of the early post-glacial era (Price and Woo, 1988c). This is overlain by 1.7–2.2 m of more recently deposited marine sediments of silt and fine sand. The topography is characterized by a low gradient of 0.001, and sub-parallel raised beaches are superimposed on the coastal plain (Fig. 1). A detailed discussion of the field and experimental methods has previously been reported (Price and Woo, 1988a,b).

MODELLING APPROACH

Points along a transect perpendicular to the prograding coastline represent successively older stages in the marsh genesis. The most recent point exists at the current mean high water (MHW) line. The position of the beach ridges relative to the MHW line is indicative of their age. With isostatic rebound occurring at 0.7–1.25 m per century (Webber et al., 1970) , the coast progrades 700–1250 m per 100 years. Based on the average rate of progradation, and the distance of each ridge beyond MHW, the first ridge (Fig. 1) is ~60 years old, and the second ridge an additional 50 years. Fairbridge and Hillaire-Marcel (1977) estimated the average time between ridge development along the Hudson Bay coast to be 45 years.

The hydrological processes currently occurring on the first beach ridge/depression are different from those occurring on the second because the more mature second ridge has an elevated surface owing to peat accumulation, and the more rapid peat formation in the inter-ridge depressions has raised the water table behind the second ridge, so that relatively fresh water cascades over it during the thawed season. Thus, at the second ridge the hydraulic head is higher, and is maintained at saturation. To reflect these differences, the simulation was done in two phases, with different initial and boundary conditions applied at each stage. The first and second phases represent the first and second beach ridge and depression sequences, respectively (Fig. 1).

Where strong gradients of chloride concentration occur, it is necessary to consider the effect of variable density on the fluid motion. For density-dependent flow (Pinder and Gray, 1977):

$$v = -\frac{k}{\mu n}(\nabla P + \rho g \nabla Z) \tag{1}$$

where k is the permeability tensor [L^2], μ is dynamic viscosity [$ML^{-1}T^{-1}$], n is porosity [1], P is pressure [$ML^{-1}T^{-2}$], ρ is density [ML^{-3}], g is the gravitational acceleration constant [LT^{-2}], and Z is the elevation [L] above a reference datum. The fluid mass balance (Voss, 1984) is then represented by:

$$\frac{d(n\rho C)}{dt} = -\nabla(n\rho v C) + \nabla(n\rho D^* \nabla C) \tag{2}$$

where C is solute concentration [M_{solute}/M_{fluid}] and D^* is the dispersion coefficient [L^2T^{-1}].

Dispersion comprises two processes: mechanical dispersion (D_m) resulting from velocity variations within the sediment matrix, and molecular diffusion(D^*) across the concentration gradient, where:

$$D = D_m + D^* \tag{3}$$

and

$$D_m = \alpha v \tag{4}$$

where α is the dispersivity [L] of the porous medium. Typically, eqn. (1) has been used to simulate the migration of leachate or contaminant plumes in aquifers (e.g. Frind and Hokkanen, 1987). In the present study this equation represents the dispersal or displacement of a solute initially present in the soil matrix.

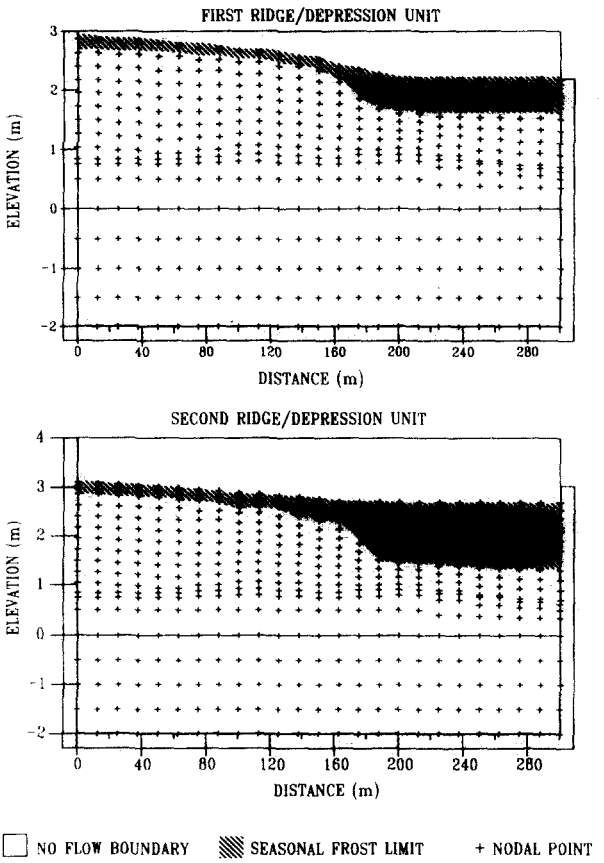

Fig. 2. Boundary conditions and nodal incidences for quadrilateral elements in the first and second ridge/depression units.

The model USGS–SUTRA (Saturated–Unsaturated Transport), contains the equations and spatial refinement required by this study. The SUTRA model employs a hybrid finite element and integrated finite difference method to approximate the governing equation (eqn. (1)), coupling fluid density-dependent flow and solute transport (Voss, 1984). Simulation can be performed using transient flow and transport, and specified pressure and/or concentration at the various nodes and boundaries.

Boundary conditions

Boundary conditions for the flow simulation are similar for both stages (Fig. 2). The model domain extends from the crest of the ridges to the centre of the depression and from the surface down to an elevation of − 2.0 m above sea level (a.s.l.). The coast is toward the right side of Fig. 2. There is a no-flow boundary on the left at the ridge crest where the flow is primarily downward. On the second ridge, field data indicate that horizontal flow occurs, but is two to three orders of magnitude less than vertical groundwater flow. The vertical no-flow boundary was assumed for simplicity. On the first ridge, field data confirm this boundary condition on all but the dry condition.

A no-flow boundary occurs on the right side between adjacent ridges (the centre of the depression), where the extremely low horizontal gradient (0.0001) across the ponded water makes lateral flow insignificant. The lower no-flow

TABLE 1

Parameters for SUTRA model simulation

Parameter	Value	Description
g	$9.8\,m\,s^{-1}$	Acceleration due to gravity
n	0.3	Porosity
K_x	$K_y\,m\,s^{-1}$	Hydraulic conductivity
K_p	$10^{-5}\,m\,s^{-1}$	Hydraulic conductivity of peat layer
K_{slt}	$10^{-7}\,m\,s^{-1}$	Hydraulic conductivity of silt (Phase 1)
K_{slt}	$10^{-6}\,m\,s^{-1}$	Hydraulic conductivity of silt (Phase 2)
K_{snd}	$10^{-6}\,m\,s^{-1}$	Hydraulic conductivity of sand
K_c	$10^{-10}\,m\,s^{-1}$	Hydraulic conductivity of clay
C_{IN}	$0\,kg\,m^{-3}$	Concentration of inflow
C_o	$0\,kg\,m^{-3}$	Base fluid solute concentration
ρ_o	$1000\,kg\,m^{-3}$	Fluid density at $C = C_o$
$\delta\rho/\delta C$	$700\,kg\,m^{-3}$	Density change with concentration
μ	$10^{-3}\,kg\,m^{-1}\,s^{-1}$	Dynamic viscosity
S_w	1	Saturation ratio
S_{op}	0	Specific pressure storativity
b	0	Compressibility of water
$a_L = a_T$	0 m	Longitudinal and transverse dispersivity
D^*	$3D^{-10}\,m^2\,s^{-1}$	Diffusion coefficient in water
D^*_{ice}	$2.5D^{-14}\,m^2\,s^{-1}$	Diffusion coefficient in ice
B	1 m	Thickness of modelled region

boundary is deep within the underlying clay, which is of low permeability (Table 1). The upper flow boundary is the water table, which is fixed at the surface. These conditions imply continuous saturation; this is valid on the second ridge. On the first ridge the water table fell by as much as 0.3 m during dry conditions, but gravimetric soil moisture analysis indicates that tension saturation occurs in all but the upper 5 cm of organic material. An arbitrary model domain thickness of 1 m is assigned to the simulated transect to maintain dimensional tractability.

The boundary conditions for the chloride transport simulation depend on the flow boundary conditions. If the specified pressure boundary at the water table requires recharge, then the concentration (C) of recharge is $C = 0\,\mathrm{kg\,m^{-3}}$. The chloride concentration of any discharge is at the ambient concentration of the aquifer fluid in the vicinity of the discharge point. Solute is not allowed to cross the no-flow boundaries, either by dispersion or by advection. This is of little consequence because solute concentration is similar on either side of the boundaries. The lower no-flow boundary is sufficiently deep to preclude significant transport in that zone.

During the first phase of the simulation, the change in concentration at all nodes was determined by eqn. (2). During the second phase, the surface concentration of the ridge was held at zero to represent continuous flushing by the overland freshwater inflow from the inland marshes.

Initial conditions

The initial pressure (P) condition was determined for the average May–August elevation of the water table along the transect. The initial chloride condition was based on the vertical concentration profile measured at the

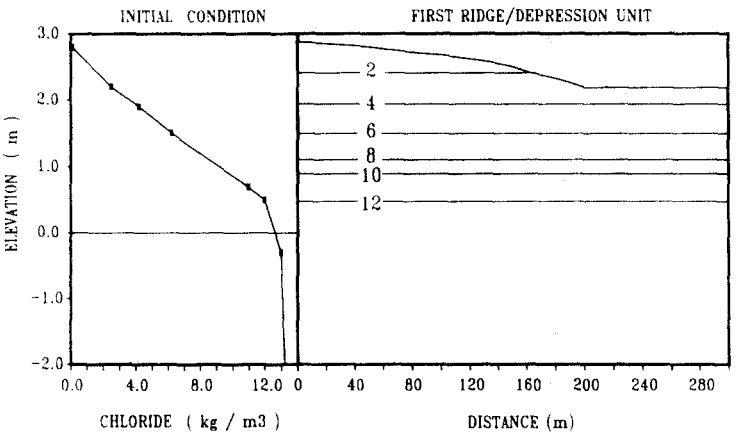

Fig. 3. Initial chloride concentration (a) in the vertical profile representing the average conditions near the MHW line; (b) in the domain of the first ridge/depression.

MHW line (Fig. 3a), which marks the earliest stage in marsh development. This profile was assigned to the mesh to produce the initial two-dimensional chloride concentration for Phase 1 (Fig. 3b).

Model assumptions

The rate and direction of flow are affected by fluid density, and it is assumed that the total dissolved solids in the fluid have the same composition as seawater. It is assumed further that tide water does not introduce any salt into the system because of the very low salinity of the local seawater (typically $< 1\,\mathrm{kg\,m^{-3}}$), and the low frequency of tidal inundation (Price and Woo, 1988b).

Dispersion (see eqn. (2)) is assumed to be a function of diffusion alone, because mechanical dispersion (eqn. (4)) is significant only where the average linear pore water velocity is large enough to raise the Peclet number above unity (Gillham and Cherry, 1982). The Peclet number (P_e) is given by:

$$P_e = vd/D^* \tag{5}$$

where d is the average particle diameter, v is the average linear pore water velocity, and D^* is the chloride diffusion coefficient. Here, 50–90% of the sediment by weight is silt ($< 37\,\mu$m), D^* is in the range of $10^{-10}\,\mathrm{m^2\,s^{-1}}$, and v is 10^{-8} to $10^{-14}\,\mathrm{m\,s^{-1}}$, so that the Peclet number is three to nine orders of magnitude below unity. Even though field scale dispersivity is much greater than that represented by d, the very low Peclet number indicates that molecular diffusion prevails as the dispersive mechanism. The diffusion coefficient in the unfrozen layer is also assumed to be independent of temperature.

Given the shallow flow system and the intense cold of the subarctic winter, the effect of seasonal frost has to be considered. Concrete frost is formed in the upper layers between December and April, and is deeper in the windswept areas which are blown clear of snow, notably in the depressions. Based on frost depth measurements from 1984 and 1985, concrete frost is mimicked in the appropriate model nodes by substituting the viscosity of ice (μ_i) for water (μ) and the chloride diffusion coefficient in ice (D^*_i) instead of water (D*). Three periods are assumed for each year: (1) six months with no frost; (2) three months at half the observed maximum depth; (3) three months at the maximum frost depth (Fig. 2). Thus, following six months with no frost, μ_i replaces μ, and D^*_i replaces D^* for the appropriate nodes for three months of simulation; then for the next three months, the other nodes representing the full frost condition are included. These parameter substitutions are made repeatedly during the simulation.

Parameterization and model mesh design

Extensive field measurements provide the requisite parameters for the system. Complex spatial distributions of parameters are often used to reproduce details of measured behaviour. However, for this model which

simulates the long-term behaviour of the marsh water and chloride fluxes, bulk parameterization is selected. Simple distribution and single parameter values are preferable if they provide good results (Souza and Voss, 1987). Thus, the average hydraulic conductivity for each soil type is used, creating a layered homogeneous isotropic domain. The average porosity is assigned throughout the modelled region. The parameter values used in the model are listed in Table 1.

The finite element mesh for the model has 500 nodes and 456 elements (Fig. 2). The spacing is least dense in the Tyrrell Sea clay zone where the flow rate is very low. For the upper layers the vertical spacing is 0.1–0.2 m. Horizontal spacing is 12.5 m. The subregion of the grid representing the peat matrix is collapsed in the first phase of the simulation and expanded to the appropriate height for the second phase. The spatial discretization is within the suggested guidelines (Voss, 1984). Temporal discretization is found to be sufficient using three-monthly time steps.

RESULTS

Figure 4 shows the results after 60 years of simulation under Phase 1

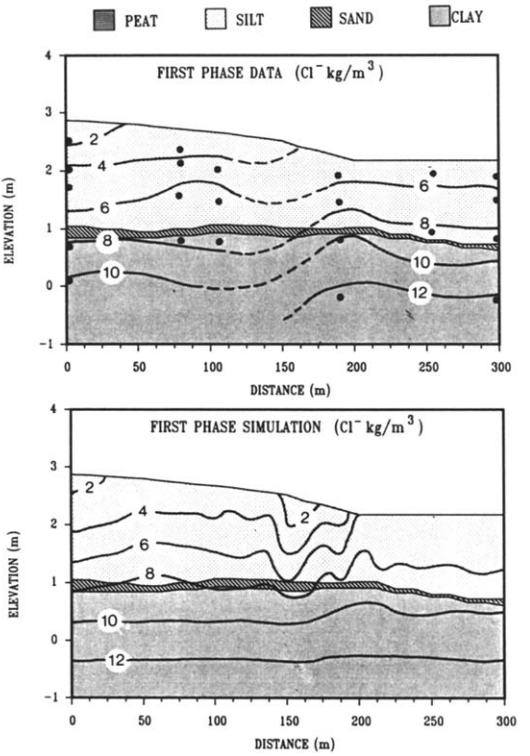

Fig. 4. Chloride distribution in the first ridge depression unit: (a) field observations; (b) simulation results.

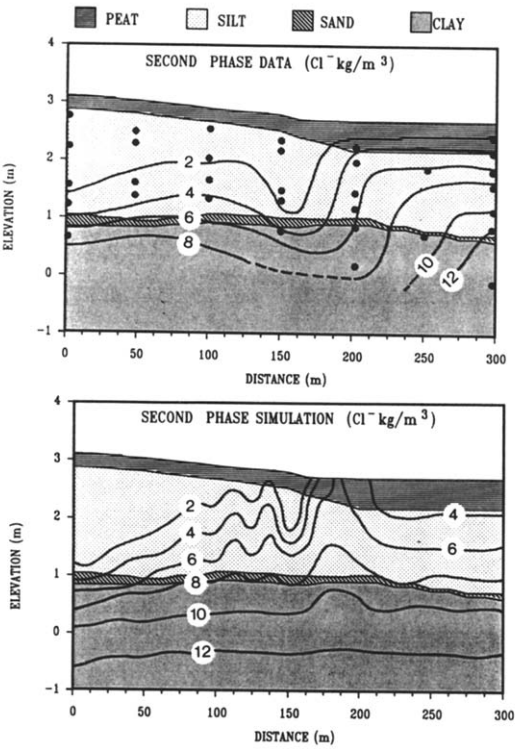

Fig. 5. Chloride distribution in the second ridge depression unit: (a) field observations; (b) simulation results.

boundary conditions, and the measured field values. The first phase of simulation results in a chloride distribution similar to the observed pattern, with lower salinity beneath the ridge owing to leaching by surface water, and elevated salinity in the depression. There is no clear demarcation of the recharge depth, as the solute front is blurred by diffusion. Strong recharge and discharge occur near the break in slope between the ridge and depression, causing the chloride concentration isolines to dip and then rise accordingly (Fig. 4). There are insufficient field data in this zone to provide a detailed pattern, but the simulated and measured values are similar. In the depression the upward water movement is weak, and chloride transport is dominated by diffusion; the simulation produces higher chloride concentrations there than the field observations but values converge rapidly to values as high as those produced by the simulation for depths exceeding 0.5 m.

The simulated chloride concentrations for Phase 1 (Fig. 4) are used as initial conditions for Phase 2. The average measured parameter values used for the second phase do not produce sufficient leaching of salt in the ridge to match the observed chlorinity, unless the strength of the vertical water fluxes is increased by an order of magnitude (Fig. 5). This has little effect on the simulated chloride

values for the depression beyond the discharge zone because of the extremely low water velocities there (10^{-14} m s^{-1}). The range of observed and simulated pore water concentrations of the ridge in the zone above the Tyrrell Sea clay are both about 0–6 kg m^{-3}. The discharge zone at the foot of the ridge marks the end of the advective transport regime, and the start of the diffusion dominant regime of the depression. The simulation yields chloride concentrations of 0–9 kg m^{-3} in the depression, compared with 0–12 kg m^{-3} measured in the field.

The simulations are repeated without the seasonal frost, and the results are indistinguishable from Figs. 4a and 5a when the simulation time is halved.

DISCUSSION

Simulation reproduces the general trend of recharge and discharge observed in the field. In the first phase of simulation, leaching of chloride from the beach ridge is slightly greater than observed; the simulated 4 kg m^{-3} isoline plots 0.05–0.10 m deeper (Fig. 4). The water table of the first ridge during the summer is frequently 0.06–0.12 m beneath the surface (Price and Woo, 1988a); this reduces the recharge produced by the fully saturated condition (i.e. water table at the surface). The distorted isochlors at the interface of the ridge and depression may have resulted from a discontinuous high permeability sand layer (Freeze and Cherry, 1979, p. 398). The oscillations in this zone are caused by adjacent recharge and discharge nodes, produced by the pressure distribution, which is very sensitive to the specified elevation of the surface nodes there. Chloride transport in the depression is primarily by diffusion, since low pore water velocity ($\sim 10^{-10}$–10^{-14} m s^{-1}) does not favour advective transport. There is no recharge here, and in the absence of a mechanism to remove the chloride at the surface during the Phase 1 simulation, concentration continues to increase to equilibrate with the higher salinity at depth. In the field, the surface is occasionally subjected to the infiltration of rainwater, so that the chloride concentration at the surface of the first depression is reduced to $\sim$ 2 kg m^{-3}.

During the second phase of simulation, the surface concentration is held at zero, maintaining a strong concentration gradient that enhances the upward chloride loss by diffusion. However, the simulated recharge based on the measured parameters is insufficient to cause the degree of leaching observed in the field. This problem arises because the groundwater transport model does not have a surface flow component to replicate the moving water above the surface. On the second ridge, surface water from inland marshes maintains a water table at 0–0.10 m above the surface for 45% of the time between May and August (which includes the driest period of the year). The higher pressure to be expected in the porous medium below is not achieved by specifying the water table at the surface. This can be overcome by experimenting with a time-dependent upper pressure boundary, or more simply by increasing the hydraulic conductivity of the silt so that the strength of recharge and discharge of the simulation matches the observed recharge and discharge (Fig. 6). The latter method has been used.

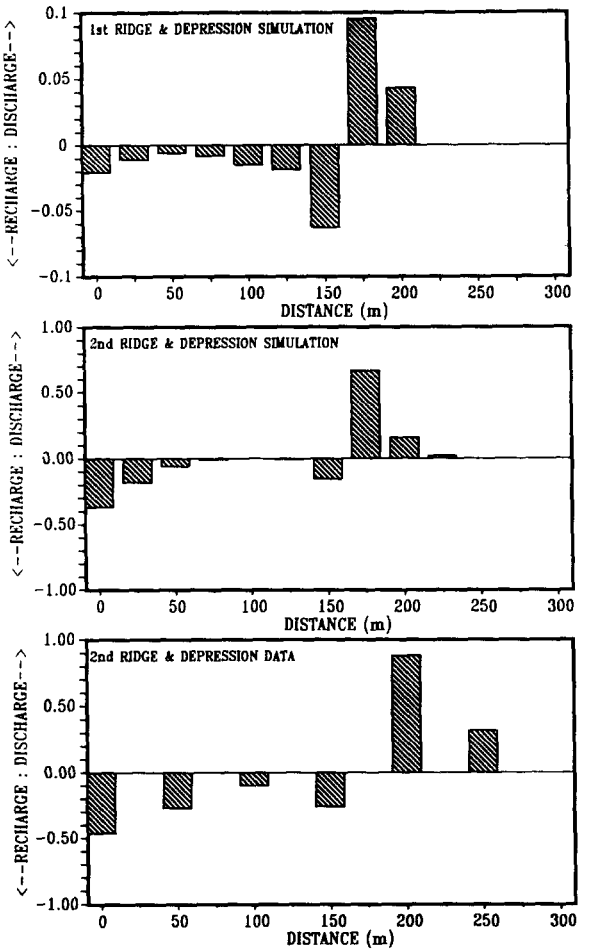

Fig. 6. Recharge and discharge: (a) simulation for first ridge/depression; (b) simulation for second ridge/depression; (c) field data for the second ridge/depression (note the scale change).

In the simulation, the chloride concentration at depth in the depression is less than the value observed in the field. This is probably caused by local spatial variation not accounted for in the initialization of the model. In spite of these incongruities, the model reproduces the trend of significantly lower concentration below the ridges.

The effect of mimicking frost in the surface layers of the wetland is to shorten the annual period of recharge/discharge by half. Doubling the simulation time achieves essentially the same result as the frost-free condition. Molecular diffusion is not affected below the frozen layer, but the advective transport processes are. The (halved) frost-free simulation does not differ appreciably from the simulation with frost conditions, suggesting that molecular diffusion is not very important over the short term.

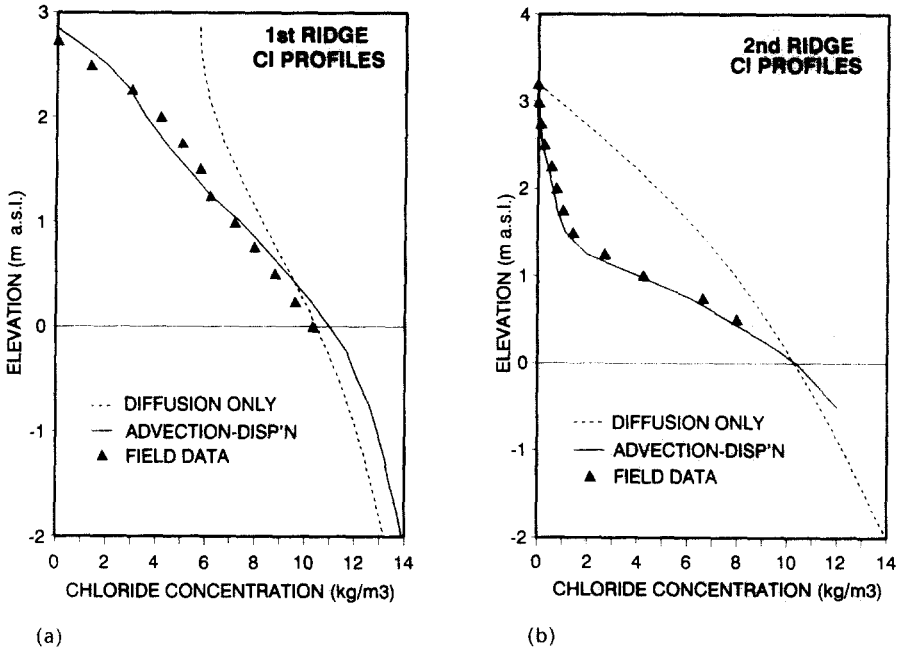

Fig. 7. Natural and simulated (advection dispersion and diffusion only) vertical chloride concentration profiles for (a) first ridge; (b) second ridge.

Advection vs. diffusion

The importance of advection in the spatial distribution of chloride can be demonstrated by comparison of the results with a diffusion-only simulation. This can be done with the SUTRA model by increasing the hydraulic conductivity many orders of magnitude, so that water flow is not significant. The results for the beach ridge sites are shown in Fig. 7, along with the SUTRA simulation previously described, and the actual chloride concentrations. The diffusion simulation of the first ridge was the initial chloride condition for the second phase (Fig. 7b).

In the first phase of the diffusion simulation, the predicted chloride concentration (Fig. 7a) diverges from actual data towards the surface, because no chloride is being lost from the system. The SUTRA simulation, however, provides a much better approximation because recharge at the upper boundary leaches salt down, more closely approximating the true field condition. The second phase result (Fig. 7b) indicates that the diffusion underestimates the rate of chloride loss, and that the SUTRA simulation more closely resembles the data, again because of leaching. Clearly, the diffusion-only simulation is inadequate to describe the short-term chloride transport regime.

ACKNOWLEDGEMENTS

The financial support of the Natural Science and Engineering Research Council, and the Department of Indian and Northern Affairs through provision of the Northern Student Training Grant is gratefully acknowledged.

REFERENCES

Casey, W.H. and Lasaga, A.C., 1987. Modelling solute transport and sulphate reduction in marsh sediments. Geochim. Cosmochim. Acta, 51: 1109–1120.

Environment Canada, 1982. Canadian Climatic Normals. Temperature and Precipitation, Ontario, Ottawa.

Fairbridge, R.W. and Hillaire-Marcel, C., 1977. An 8000-yr paleoclimatic record of the 'Double-Hale' 45-yr solar cycle. Nature, 268: 413–416.

Freeze, R.A. and Cherry, J.A., 1979. Groundwater. Prentice-Hall, Englewood Cliffs, NJ, 604 pp.

Frind, E.O. and Hokkanen, G.E., 1987. Simulation of the Borden plume using the alternating direction Galerkin technique. Water Resour. Res., 23: 918–930.

Gillham, R.W. and Cherry, J.A., 1982. Contaminant migration in unconsolidated geological deposits. Geol. Soc. Am. Spec. Pap. 189.

Pinder, G.F. and Gray, W.G., 1977. Finite Element Simulation in Surface and Subsurface Hydrology. Academic Press, New York, 295 pp.

Price, J.S. and Woo, M.K., 1988a. Studies of a subarctic coastal marsh. I. Hydrology. J. Hydrol., 103: 275–292.

Price, J.S. and Woo, M.K., 1988b. Studies of a subarctic coastal marsh. II. Salinity. J. Hydrol., 103: 293–307.

Price, J.S. and Woo, M.K., 1988c. Origin of salt in Hudson and James Bay coastal marshes. Can. J. Earth Sci., 25: 145–147.

Price, J.S., Ewing, K., Woo, M.K. and Kershaw, K., 1988. Vegetation patterns in James Bay coastal marshes: II. Effects of hydrology on salinity and vegetation. Can. J. Bot., 66: 2586–2594.

Souza, W.R. and Voss, C.I., 1987. Analysis of an anisotropic coastal aquifer system using variable-density flow and solute transport simulation. J. Hydrol., 92: 17–41.

Voss, C.I., 1984. SUTRA — Saturated Unsaturated Transport. A finite-element simulation model for saturated–unsaturated, fluid-density dependent ground-water flow with energy transport or chemically reactive single-species solute transport. U.S.G.S., National Center, Reston, VA, 409 pp.

Webber, P.J., Richardson, P.W. and Andrews, J.T., 1970. Post-glacial uplift and substrate age at Cape Henrietta Maria, southeastern Hudson Bay, Canada. Can. J. Earth Sci., 7: 317–325.